IPPI
Polyolefins Journal, Vol. 11, No. 2 (2024)
DOI: 10.22063/POJ.2024.3519.1284
ORIGINAL PAPER

Synthesizing polypropylene with percolation network catalyzed by inorganic nanoparticles-functionalized Ziegler-Natta catalyst

Tingting Yang[1, 2,*], Ao Li[1, 3], Yawei Qin[4], Jin-Yong Dong[4,*]

[1]Taiyuan University of Technology, Taiyuan, Shanxi 030024, China
[2]Shanxi Coking Coal Group Co., LTD, Taiyuan, Shanxi 030024, China
[3]Jinneng Holding Group, Datong, Shanxi037000, China
[4]CAS Key Laboratory of Engineering Plastics, Institute of Chemistry, Chinese Academy of Sciences, Beijing 100190, China

Received: 31 October 2023, Accepted: 31 January 2024

ABSTRACT

Polypropylene is one of the most widely used synthetic resins, which is mainly synthesized with Ziegler-Natta catalysts. In this paper, the functionalized Ziegler-Natta catalyst is applied to prepare high-performance polypropylene. A new way to synthesize functionalized Ziegler-Natta catalysts is to dope with inorganic nanoparticles. The $MgCl_2/TiCl_4$/BMMF catalysts doped with halloysite nanotubes were prepared and applied to synthesize polypropylene containing less than 200 ppm halloysite nanotubes. It is found that doping nanotubes in Ziegler-Natta catalyst has little impact on the structure, composition and activity of the catalyst, and polypropylene with high isotactic degree and molecular weight was synthesized with the functionalized Ziegler-Natta catalyst. Halloysite nanotubes are found to be dispersed in polypropylene in the form of individual nanotube, forming percolated network in the polymer melt effectively. Moreover, the polypropylene containing halloysite nanotubes exhibited better mechanical and thermal resistance properties as compared with conventional polypropylene, and the thermo-oxidative properties of which do not deteriorate as the introduction of nanotubes. This research provides a facile way to relieve the contradiction between the high activity of catalyst and high content of nanoparticles during the preparation of polyolefin nanocomposites by in-situ polymerization, and a new idea to prepare polyolefin nanocomposites by in-situ polymerization. **Polyolefins J (2024) 11: 83-93**

Keywords: Ziegler-Natta catalyst; polypropylene; halloysite nanotubes; doping in situ; percolation network.

INTRODUCTION

Isotactic polypropylene (PP) is widely used in industry due to its well-balanced physical and mechanical properties and its easy processability at a relatively low cost [1,2]. However, its relatively poor impact strength restricts its application as an engineering thermoplastic [1,3]. Therefore, the research in modified PP, has been a hot topic in the material field. Polymer nanocomposites are promising materials, in which a small fraction of nanoparticles dispersed in polymer matrices not only induces drastic reinforcements but also enhances functionalities such as conductivity and gas barrier properties [4]. When the polymer is stressed, the rigid nanoparticles in the matrix act as the stress concentration points, and the surrounding polymer deforms plastically, thus consuming a large amount of energy and achieving the purpose of toughening the polymer.

The commonly used preparation methods for polymer nanocomposites include: blending method (solution blending and melt blending), in-situ method, in-situ

*Corresponding Author - E-mail: jydong@iccas.ac.cn, yangtingting@tyut.edu.cn

intercalation method, radiation synthesis method, and sol-gel method [5]. The in-situ intercalation method is an important method for the preparation of polymer/clay nanocomposites. It involves inserting monomers or polymers into the clay layers, destroying the lamellar structure of the clay, so that the clay layer is dispersed in the polymer with about 1nm thickness. The in-situ preparation method can reduce the agglomeration of nanoparticles in polymer and achieve uniform dispersed polyolefin nanocomposites. A novel reactor granule technology is reported for the preparation of polyolefin nanocomposites, which involves in-situ generation of nanoparticles in the porosity of polymer reactor granule [6,7]. The nanoparticles are mainly metal compounds that can be synthesized in situ. In addition, the main in-situ method adopts the way that supporting catalysts (metallocene and Ziegler-Natta catalysts) on the surface of nanoparticles, then polymers grow on the surface of nanoparticles that bear catalytic ability. However, in the process of preparing polypropylene nanocomposites by in-situ polymerization, there is a contradiction between the loading amounts of nanoparticles and the activity of the catalyst [8-10].

Kaminsky *et al.,* [11] prepared polypropylene/silica nanocomposites and polypropylene/multi-walled carbon nanotubes (MWCNT) nanocomposites in situ catalyzed by metallocene catalyst supported on nanoparticles. Wang Ning *et al.,* [12] reported that the polypropylene/multi-walled carbon nanotubes nanocomposites exhibited good interface compatibility which are prepared by Ziegler-Natta catalyst supported on multi-walled carbon nanotubes in situ.

Yang *et al*., [8] prepared polypropylene/montmorillonite nanocomposites catalyzed by metallocene catalyst supported on montmorillonite sheets in situ. Huang *et al.,* [13] firstly prepared polypropylene/graphite oxide (GO) nanocomposites in situ catalyzed by Ziegler-Natta catalyst supported on graphite oxide sheets. The in-situ polymerization method overcomes the obstacle that GO cannot be dispersed in PP matrix uniformly due to the incompatibility between polar GO and non-polar PP matrix. Due to the morphology replication effect of polymer on catalyst, the above-mentioned method of preparing nanocomposites catalyzed by the catalyst supported on the nanoparticles cannot control the polymer morphology. It is reported that the polyolefin nanocomposites with control spheroid polymer particle morphology can be prepared in situ by the nano-supported catalyst supported on the spheroid nanoparticles reformed by the spray drying technology [14].

As a new type of one-dimensional natural nanomaterials, HNTs have the characteristics of tubular nanostructure, large specific surface area, natural availability, versatility, good biocompatibility and high mechanical strength, which make them suitable for the low-cost preparation of HNTs/polymer nanocomposites [15,16]. Most of the HNTs are microtubular structures consisting of 20-30 layers of silicate flakes of kaolin under natural conditions. The chemical composition is the same as that of kaolin, and the molecular formula is $Al_2Si_2O_5(OH)_4nH_2O$ [17]. The HNTs lamellae consist of a regular arrangement of silica-oxygen tetrahedra in the outer layer and aluminum-oxygen octahedra in the inner layer, with free water molecules between the lamellae [18]. The length of HNTs nanotubes is 0.2-2 μm, the size of outer diameter of tubes is 40-70 nm, the size of inner diameter of tubes is 10-40 nm, and the length-to-diameter ratio (L/D) is 10-50 [17-21].

In addition to, most of the halloysites have a complete shape and stable size distribution, a hollow, tubular structure and different inner and outer surface properties, which make it good reproducibility and catalytic activity. So, HNTs can be used as a raw material for catalyst carriers in the petrochemical field [22-24].

Herein, we propose a novel in-situ strategy for PP-based nanocomposites using Ziegler-Natta catalyst doped with nanoparticles. Polypropylene nanocomposites with less than 200 ppm of halloysite nanotubes (HNTs) were prepared in situ by HNTs-doped Ziegler-Natta catalyst. The composition and morphology of as-prepared catalyst, the rheological behavior of polymer melt, the thermal stability and mechanical properties of polymer were fully studied. The results indicated that polypropylene resins with ppm-level HNTs exhibited outstanding properties.

EXPERIMENTAL

Materials

All chemicals used in the preparation of HNTs-doped $MgCl_2/TiCl_4$ catalyst were analytically pure and purchased from Sinopharm Chemical Reagent, Beijing. *n*-Decane, *n*-hexane, isooctanol, tetrabutyl titanate, and diisobutyl phthalate (DIBP) were dried and stored over molecular sieve. n-Hexane was further purified by refluxing over sodium metal under

nitrogen for 48 h before use. Halloysite was obtained from Hebei Province in China. Propylene gas of research grade was purchased from Beijing Yanshan petrochemical company, China. Triethylaluminum (TEA) (Albermarle Corporation) as cocatalyst and diphenyldimethoxysilane (DDS) (Tokyo Kasei Kogyo Co.) as external electron donor were diluted in n-heptane with 1.8M and 0.088M, respectively.

Synthesis of functionalized Ziegler-Natta catalyst doped with halloysite in situ

The halloysite was calcined at 600°C for 4 h to remove the interlaminar moisture of the lamella. $MgCl_2$ powders (5 g) were dispersed in decane (40 mL) and isoctyl alcohol (24 mL) solution in N_2 atmosphere, and the mixture was subsequently headed for 2 h at 130°C. Then, tetrabutyltitanate (0.75 mL) was added into above mentioned solution and stirred for 1 h at 130°C. Diisobutyl phthalate (1.5 mL) was added and stirred for 1 h at 130°C. Finally, $MgCl_2$ alcohol containing halloysite was prepared by adding halloysite into above solution and stirred at room temperature (RT).

$TiCl_4$ (160 mL) was added into the custom-made catalyst reactor and cooled to -20°C in alcohol bath. The above prepared $MgCl_2$ alcohol containing halloysite was dropwise added into the reactor and stirred for 1 h at -20°C. After returning to room temperature slowly by removing the alcohol bath, the solution was heated to 60°C slowly. Then, fluorine diether solution (2.36 g) was added and heated for1.5 h at 110°C. The unreacted $TiCl_4$ was filtered out, and $TiCl_4$ (160 mL) was added again and stirred at 110°C for 1.5 h. Then, the obtained product was washed for 5 times using hexane. Finally, the catalyst powders were stored in glove box after drying in vacuum environment.

Synthesis of polypropylene nanocomposites catalyzed by functionalized Ziegler-Natta catalyst

The polymerization was carried out by liquid phase bulk polymerization. At normal temperature and pressure, H_2 was poured into a 2 L autoclave, and then liquid propylene (250 g), TEA (4 mL), DDS solution (0.1 mL), and HNT-doped Ziegler-Natta catalyst (18 mg) were added successively. Another liquid propylene (200 g) was added from the catalyst feed port to ensure that the catalyst is fully incorporated into the reactor. The mixture was subsequently heated for a period of time at 70°C by the polymerization. Finally, the unreacted propylene is released to terminate the polymerization. The polymer was dried by vacuum drying at 60°C.

Characterization and measurements

The structure of halloysite was measured by the Fourier infrared spectrometer (FTIR TENSOR-27, Bruker) using the transmissive mode. The Ti content of functionalized catalyst was measured by the UV spectrophotometer (721). The internal electron donor content of the catalyst was determined by gas chromatograph (Perkin Elmer Clarus 580). The specific surface area and pore volume of the catalyst were determined by the specific surface area and pore size analyzer (NOVA 2000, Quantachrome Instruments). The crystal shape of the halloysite, catalyst and polymer was determined by the X-ray diffractometer (XRD, Rigaku-2500X, λ= 0.1542 nm) using Cu Kα radiation.

The dispersion morphology of halloysite nanoparticles in polymer was characterized using the solution film formation technique as follows: a certain amount of PP-HNTs resin was taken and dissolved in boiling xylene at a concentration of 0.2 g/100 mL. Then, a drop of the above xylene solution was taken and placed on a slide with 200°C, and the slide was placed on a rotating hot stage with a speed of 2000 rpm for 1 min. Finally, the obtained polymer film was sprayed with gold, and the dispersion morphology of HNTs in the polymer was observed by scanning electron microscopy.

Isotacticity index of polypropylene (I.I) is defined as the mass ratio of the heptane insoluble polypropylene (w_2) and the polypropylene before heptane extraction (w_1). The extraction experiment was carried out by boiling n-heptane solution in a Soxhlet extractor for 12 h. The extracted substance was dried in vacuum for 24 h. The value of I.I can be calculated from the equation:

$$I.I\ (\%) = [w_2/w_1] \times 100 \quad (1)$$

The viscosity-average molecular weight of polypropylene (M_η) was measured by an Ubbelohde viscometer using decalin at 135°C. The value of M_η can be evaluated by Mark-Houwink equation as follows:

$$[\eta] = K M_\eta^{\alpha} \quad (2)$$

Herein, $K = 1.1 \times 10^{-4}$, $\alpha = 0.8$, and $[\eta]$ is the viscosity of polymer.

RESULTS AND DISCUSSION

The composition, structure and polymerization behavior of functionalized Ziegler-Natta catalysts

Figures 1 (a-d) display the scanning electron microscopy (SEM) images and the transmission electron microscopy (TEM) images of HNTs and 600°C-heated HNT (Hal-600), which clearly show that the HNTs exhibit the hollow tubular structure of 15 nm in inner diameter, 70 nm in outer diameter and 1μm in length. The halloysite nanotubes are severe agglomeration and the nano-tubular structure remains intact after high-temperature calcination. The Fourier transform infrared spectroscopy (FTIR) results of halloysite and halloysite calcined at 600°C are shown in Figure 1(e). The peaks at 3691 cm^{-1} and 3616 cm^{-1} represent the stretching vibration of hydroxyl groups (-OH) on the inner surface of halloysite nanotubes. The peak at 911 cm^{-1} is the deformation vibration of Al-O-H groups inside halloysite nanotubes [25]. The peak at 1635 cm^{-1} is the water absorption peak of halloysite. The peaks at 1112 cm^{-1}, 1024 cm^{-1}, 756 cm^{-1}, and 688 cm^{-1} represent characteristic peaks of the stretching vibration of Si-O bonds. By comparing the FTIR spectra of halloysite before and after calcination, it can be known that the basic framework of halloysite is still maintained after calcination. However, due to the absence of peaks at 3691 cm^{-1}, 3616 cm^{-1}, 1635 cm^{-1} and 911 cm^{-1}, it can be concluded that high temperature causes some of the inner surface hydroxyl groups and adsorbed water to be removed from halloysite. As FTIR is unable to provide a clearer characterization of the hydroxyl group in the high wavenumber region, we refer to the results from diffuse reflectance Fourier transform infrared spectroscopy (DR-FTIR) in the literature [25], which indicate that when the calcination temperature reaches 600°C, the Al-OH on the inner surface of the halloysite nanotubes is removed, the tetrahedral silicon-oxygen and octahedral aluminum-oxygen structures are separated and the Si-OH appears on the outer surface of the nanotubes. The wide-angle X-ray diffraction (WXRD) curve in Figure 1(f) shows that the characteristic (001) peak of halloysite is 8.68° and becomes a broad peak after calcination, mainly attributed to the dehydroxylation reaction and the formation of amorphous product (transform halloysite) during the temperature rise. The test results are consistent with the literature [25].

A schematic diagram of the preparation of functionalized Ziegler-Natta catalysts is shown in Figure 2. The calcined halloysites were doped with the $MgCl_2$ alcohol compound, and the alcohol compound reacted with the Si-OH on the outer surface of the halloysites, so that the carrier $MgCl_2$ alcohol compound was complexed on the surface of halloysite. $TiCl_4$ was added as the active component and precipitant, and the excess $TiCl_4$ reacted with the $MgCl_2$ alcohol complex to de-ethanolize and precipitate the $MgCl_2$, while $TiCl_4$ was directly loaded on the $MgCl_2$, and the precipitation of the $MgCl_2$ carrier was carried out

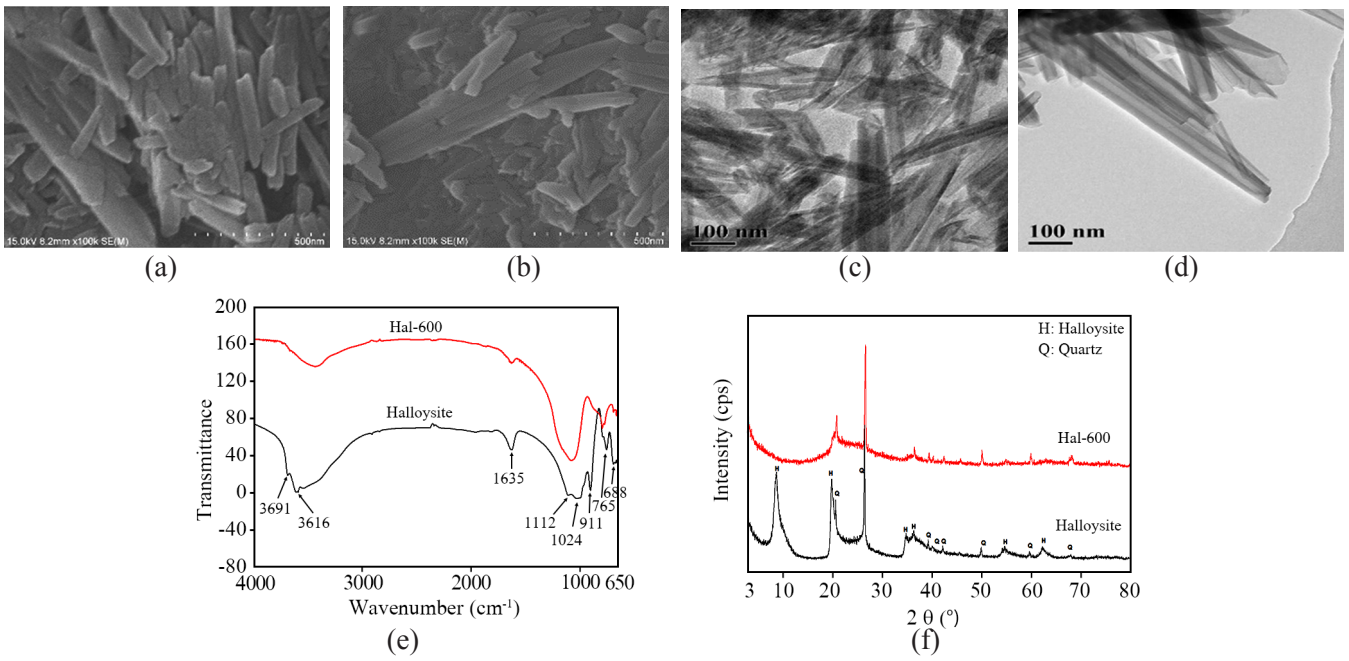

Figure 1. (a-b) SEM images of HNTs and 600°C heated HNTs; (c-d) TEM images of HNTs and 600°C heated HNTs; (e) FT-IR spectra of HNTs and 600°C heated HNTs (Hal-600); (f) WAXD profile of HNTs and 600°C heated HNTs (Hal-600).

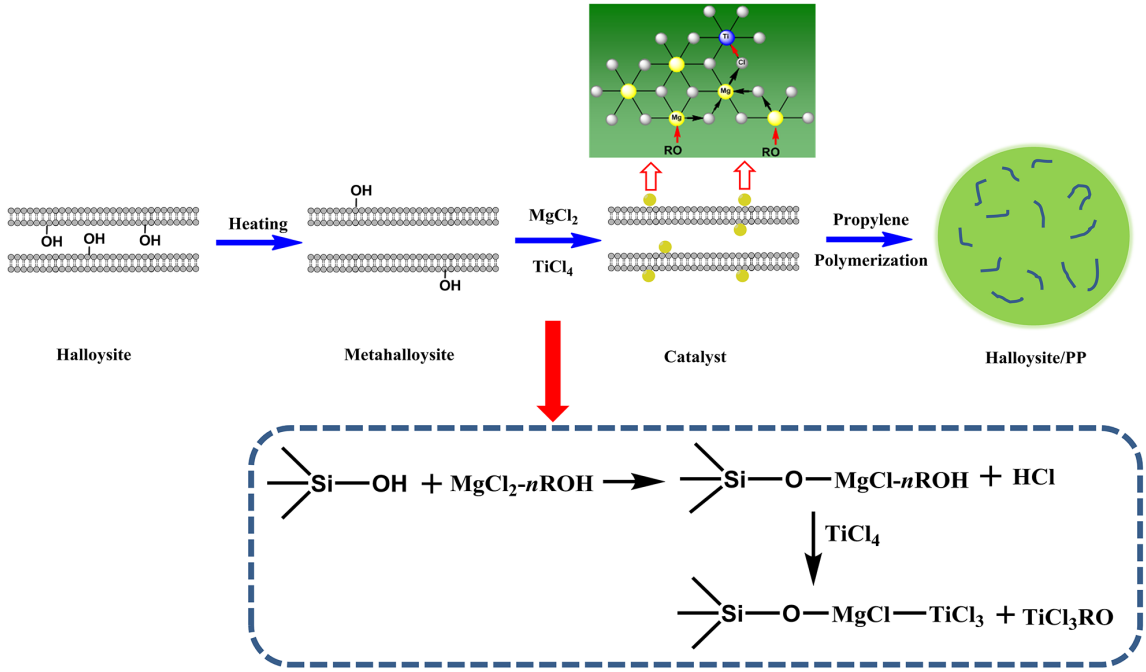

Figure 2. The preparation of Ziegler-Natta catalyst doped with halloysite in situ.

in tandem with the Ti loading process. Finally, the functionalized Ziegler-Natta catalyst was obtained. The components and results of N_2 adsorption-desorption test of the HNTs-doped Ziegler-Natta (H-d-ZN) catalyst are shown in Table 1. The content of halloysite in the H-d-ZN catalyst is 23.2 wt%, and the Ti% is 2.22 wt. %. The SEM images (Figure 3(a-b)) display the H-d-ZN catalysts possess a typical granular topography with the size of 15-20 μm, and the HNTs are embedded in the interior of H-d-ZN catalysts. X-ray diffractometry (XRD) profile in Figure 3(c) shows the characteristic peaks (15°, 32°, 50.5°) of $MgCl_2$ in the Z-N catalysts and H-d-ZN catalysts. Figure 3(d-e) shows the catalytic kinetic behavior of the Z-N catalysts and H-d-ZN catalysts at different temperatures. The polymerization rate decays rapidly and then tend to stable during the polymerization process. Compared to Z-N catalyst, the H-d-ZN catalyst exhibits a slower decay rate and a faster polymerization rate at the same temperature. It can be concluded that the doping of HNTs has little effect on the morphology, the crystal structure and the polymerization behavior of the catalyst.

The structure and performance of polypropylene resins

PP-HNTs resins with different HNT contents (0-168ppm) and different polymer molecular weights were prepared by adjusting the polymerization reaction time and hydrogen pressure for propylene polymerization catalyzed by HNT-doped Ziegler-Natta catalyst. Table 2 shows the polymerization conditions and some of the properties of PP-HNTs resins. Compared to commercial Ziegler-Natta catalyst (control-1), the HNT-doped Ziegler-Natta catalyst (Sample-1) exhibited higher polymerization activity at the same hydrogen pressure. With the decrease of H_2, the activity of catalyst decreased, the molecular weight of polymers increased, and the isotacticity index of polymers was not influenced noticeably. It has been proposed in the literature that the dormant active species of chain propagation will be activated with the addition of H_2, leading to the enhancement of catalyst activity [26,27]. The decrease of polymer molecular weight with the increase of H_2 ascribes to the occurrence of chain transfer to H_2.

Figure 4 (a-b) display the SEM images of the prepared PP-HNTs resin and PP resin, which show that both the

Table 1. The components and results of N_2 adsorption-desorption test of the HNTs-doped Ziegler-Natta catalyst.

Catalyst	Internal electron donor (i-Donor)	Catalyst components				N_2 adsorption-desorption test		
		Ti% wt.%	Mg% wt.%	i-Donor% wt.%	Hal% wt.%	S_{BET} m²/g	V cm³/g	D nm
H-d-ZN	BMMF	2.22	11.74	9.16	23.2	33.71	0.0821	9.743

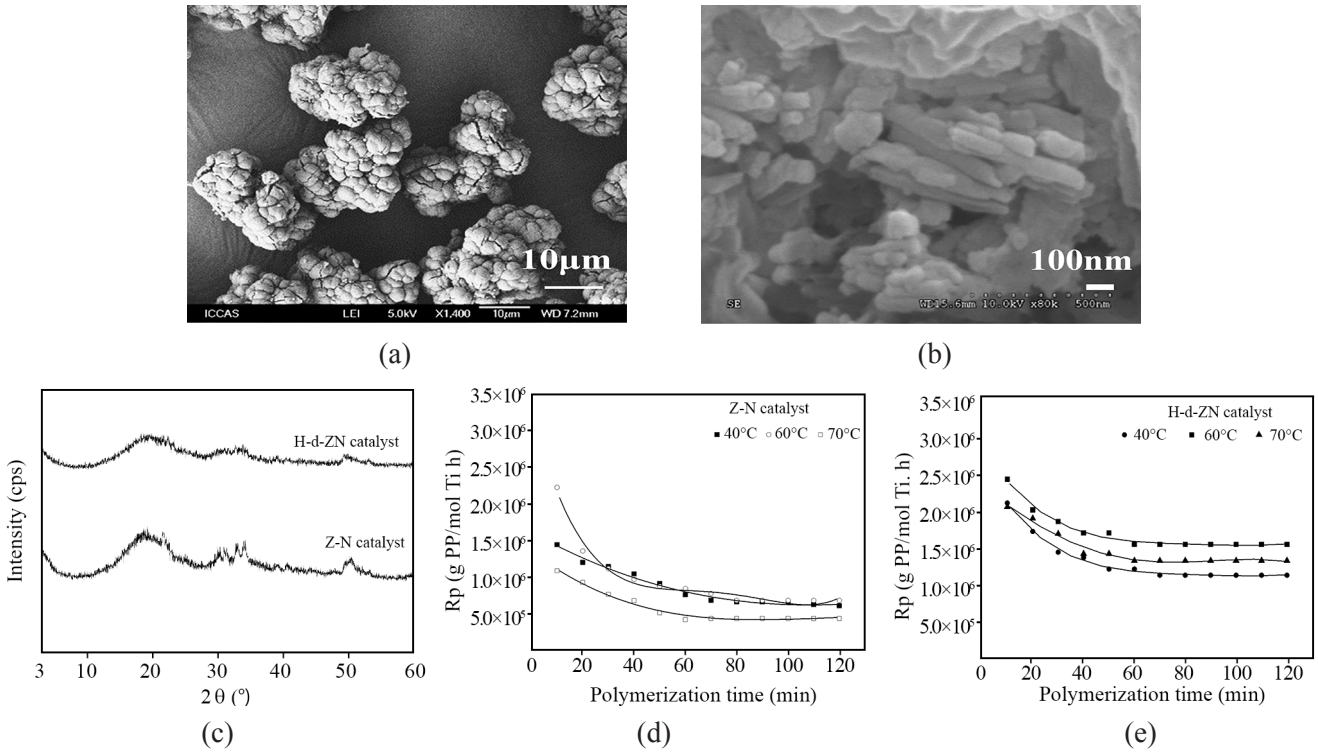

Figure 3. (a-b) SEM images of HNTs-doped Ziegler-Natta catalyst; (c) WAXD profile of a HNTs-free standard Ziegler-Natta (Z-N) catalyst and HNTs-doped Ziegler-Natta (H-d-ZN) catalyst; (d-e) The time rate profiles of polymerization at 40-70°C by a HNTs-free Ziegler-Natta catalyst and HNTs-doped Ziegler-Natta catalyst.

PP-HNTs and PP resin exhibit the particle morphology with the average size of 500 μm. To investigate the dispersion of HNTs in the PP-HNTs resin, the SEM image with the solution film-forming technique is provided (Figure 4(c)). HNTs in the PP-HNTs resin exist as individual particle without agglomeration. We can conclude that HNT-doped Ziegler-Natta catalyst shows high polymerization activity, and the resulting PP-HNTs resin has controlled morphology, high isotacticity and high molecular weight.

XRD pattern in Figure 5 (a) shows that the characteristic (300) peak (15.9°) appears in PP-HNTs resin, indicating that HNTs can induce the generation of β-crystals in the polypropylene. To investigate the microstructure of PP-HNTs resin, the small amplitude oscillation shear test was carried out and the dynamic rheological curves are provided in Figure 5(b-d). According to the linear viscoelastic theory [28], G' and $G''$of linear polymer meet the laws which are $G'\sim\omega^2$ and $G''\sim\omega^1$ in the low shear frequency region. As shown in Figure 5(b-d), the G' of PP resin meets the law, while that of PP-HNTs resin deviates from the law and tends to form a platform in the low shear frequency region. This is attributed to the formation of

Table 2. Propylene polymerization with HNT-doped Ziegler-Natta catalyst and the properties of the corresponding PP-HNTs resins.

Sample	H_2 (MPa)	t (min)	Yield (g)	Activity ($kg_{PP}\cdot g_{cat}^{-1}\cdot h^{-1}$)	$w_{(HNT)}$ (10^{-6})	*I.I.* (%)	M_η ($\times10^4 g\cdot mol^{-1}$)
Control-1	0.10	60	360	24.0	--	95.0	28.8
1	0.10	20	200	28.5	20	97.2	28.0
2	0.07	60	70	5.0	43	97.0	45.8
3	0.08	15	50	14.4	56	98.3	31.2
4	0.04	30	60	5.6	73	97.1	75.1
5	0.08	5	25	14.2	168	98.5	29.7

Polymerization conditions: 450 g liquid propylene, 5 mL triethyl aluminum (TEA, 1.8 mol/L *n*-heptane solution), 4 mL diphenyldimethoxysilane (DDS, 0.0088mol/L *n*-heptane solution); Temperature: 70°C Control-1: prepared with a commercial Ziegler-Natta catalyst without halloysite nanotubes (HNT). t: polymerization time. $w_{(HNT)}$: the content of HNT in polypropylene. T_m: melting temperature. ΔH_m: melting enthalpy. *I.I.*: isotacticity index. M_η: viscosity-average molecular weight. PP-HNTs: polypropylene resins containing HNTs.

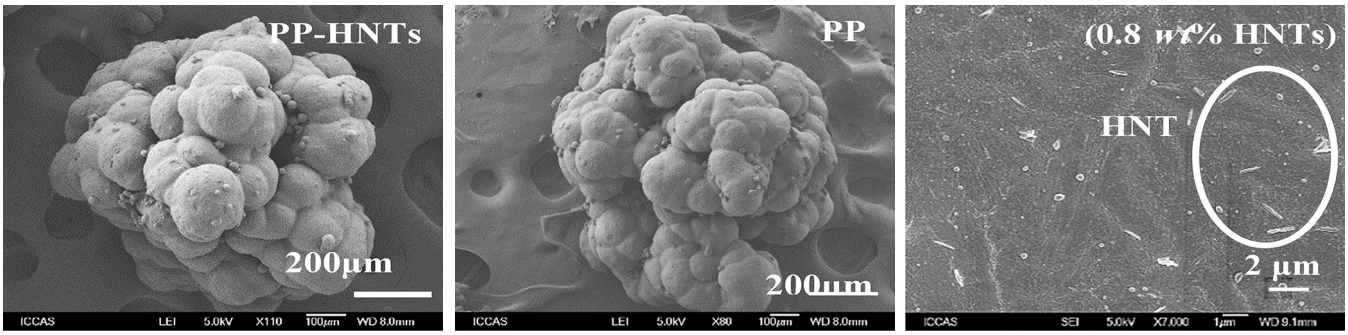

(a) (b) (c)

Figure 4. (a-b) SEM images of PP-HNTs resin and PP resin; (c) SEM image of a typical PP-HNTs resin (0.8 wt% HNT) after solution film-forming.

percolation network of HNTs nanoparticles in the PP-HNTs resin [29,30], which restricts the movement of polymer molecular chains. The hydrodynamic volume of nanoparticles overlaps when the distance between nanoparticles is close, resulting in the enhanced interaction and the formation of percolation network of nanoparticles. Meanwhile, the *G′* of PP-HNTs resin is higher than that of PP due to the enhancement effect of HNTs.

The thermal stability of PP resin can be improved by introducing nanoparticles. The thermal gravimetric analysis (TGA) curves and data of PP and PP-HNTs resin measured in N_2 are provided in Figure 6(a) and Table 3. It is noteworthy that compared with PP resin, the thermo-decomposed temperature of PP-HNTs resin with 43 ppm HNTs has increased by 44°C of

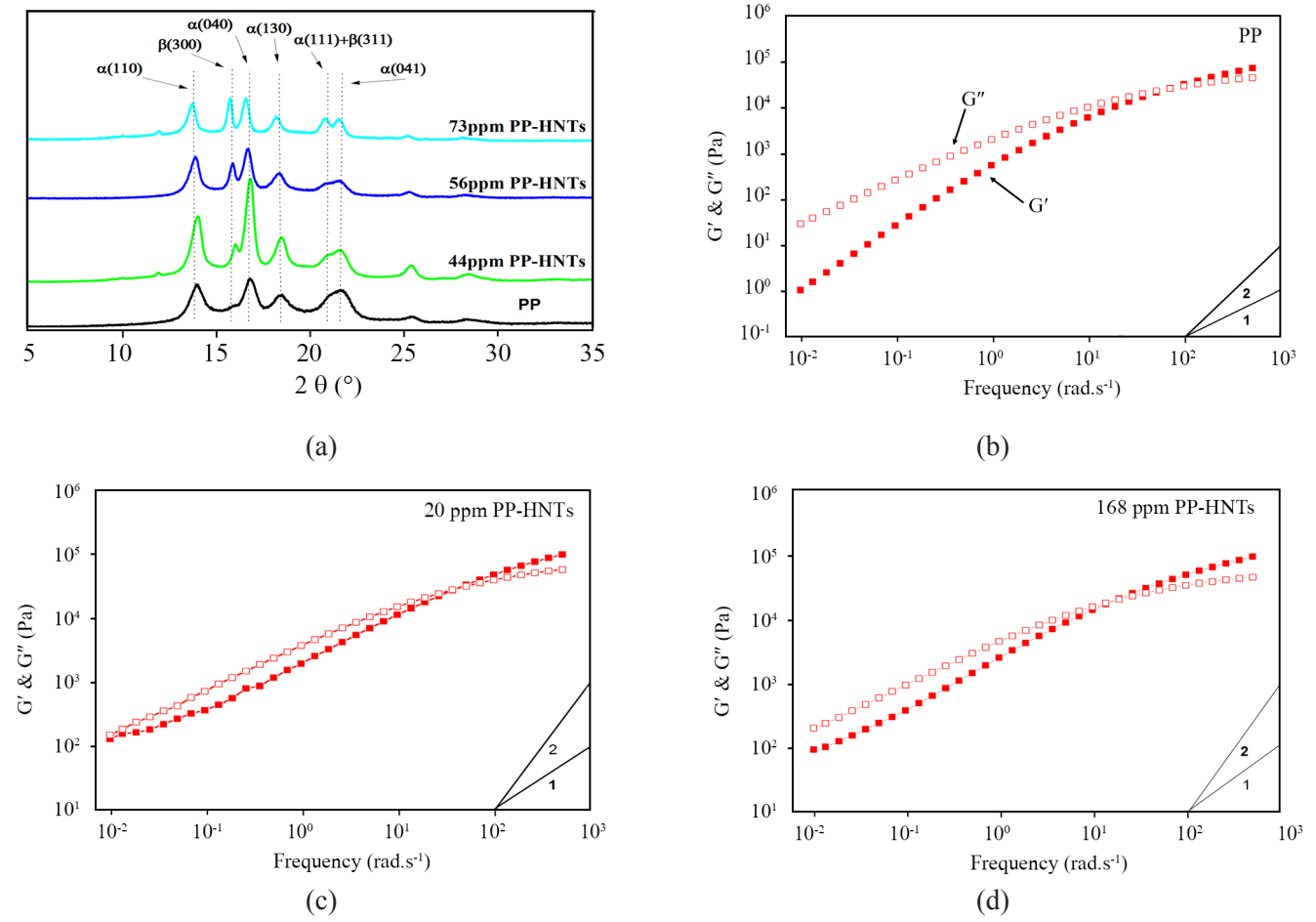

(a) (b) (c) (d)

Figure 5. (a) XRD pattern of compression-molded PP and PP-HNTs resin; (b-d) Dynamic rheological curves of PP-HNTs resin, ■ G′: Storage modulus, □ G″: Loss modulus.

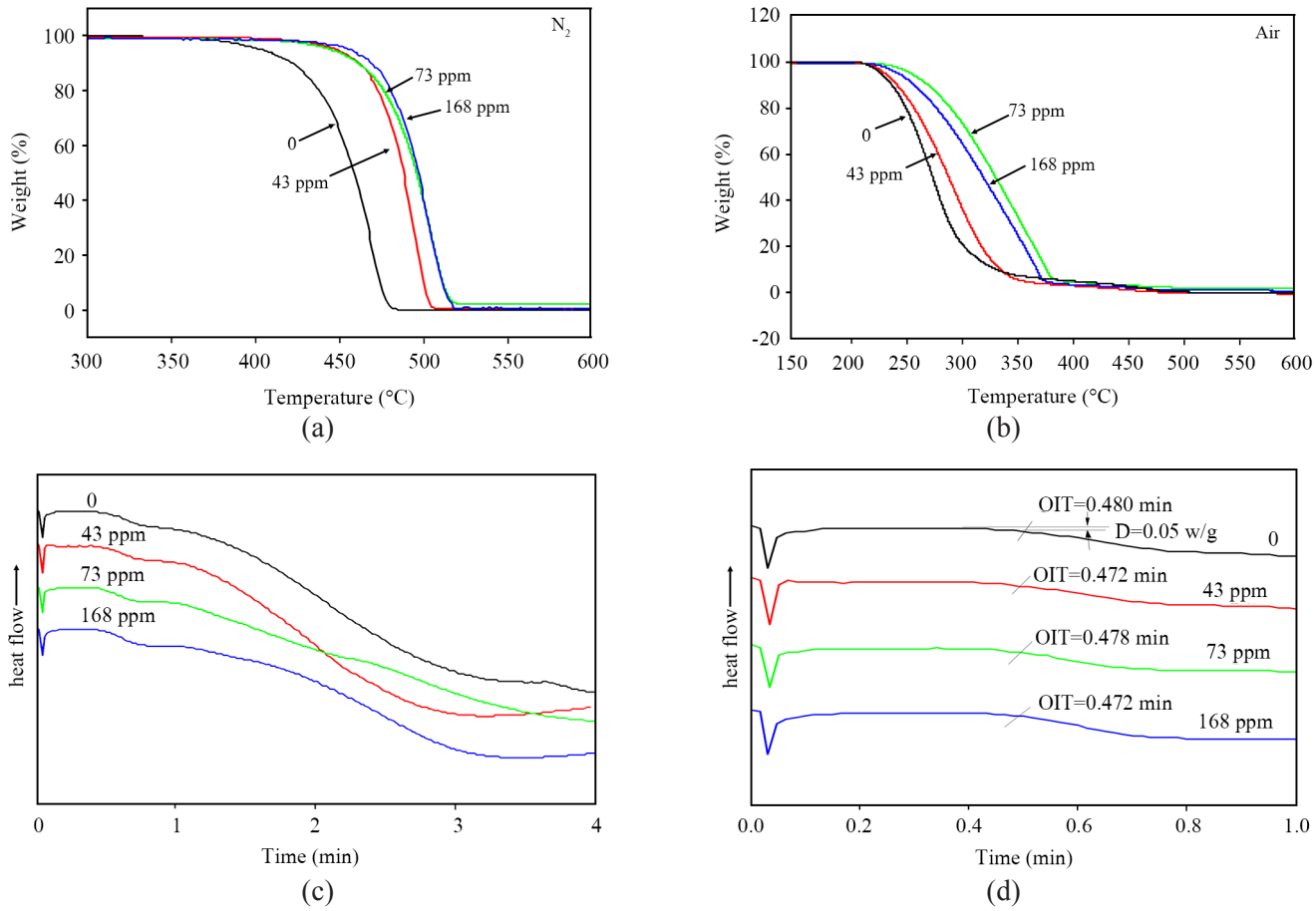

Figure 6. (a-b) TGA curves of PP and PP-HNTs resin measured in N_2 and air; (c-d) Curves of oxidation induction time (OIT) of PP and PP-HNTs resins.

5% weight loss, 40°C of 10% weight loss, and 27°C of maximum mass loss rate in N_2. It is a much larger increase than that of PP/HNTs composites reported in the literature [31]. It indicates that by the mean of doping HNTs into Ziegler-Natta catalyst, the finely dispersed HNTs in PP-HNTs resin fully develop their thermal barrier nanometer effect.

Meanwhile, the thermal gravimetric analysis (TGA) curves and data of PP and PP-HNTs resin measured in air are provided in Figure 6(b) and Table 4. Compared with PP resin, the thermo-decomposed temperature of PP-HNTs resin with 73 ppm HNTs has increased by 27°C of 5% weight loss, 32°C of 10% weight loss, and 101°C of maximum mass loss rate in air. The thermal barrier nanometer effect of HNTs can isolate oxygen, leading to the significant reduction of the decomposition rate of PP-HNTs resin.

In the processing and use, polymer material is prone to aging caused by illumination, electronics and heat, which worsen its appearance, performance and physical mechanical properties. Generally, acidic spots on the surface of clay-based fillers can cause the thermal oxygen aging of polymer [32,33]. So, to investigate the thermal and oxygen aging properties of PP-HNTs resin, the curves of oxidation induction time (OIT) of PP and PP-HNTs resins are offered in Figure 6(c-d). The thermal oxidation process includes oxidation induction stage and oxidation stage. Figure

Table 3. TGA data of PP and PP-HNTs resins measured in N_2.

Sample	$w_{(HNT)}$/ppm	$t_{0.05}$/°C	$t_{0.1}$/°C	t_{max}/°C
PP	0	404	422	469
PP-HNTs	43	448	461	496
PP-HNTs	73	445	461	504
PP-HNTs	168	456	469	504

$t_{0.05}$: temperature of 5% weight loss; $t_{0.1}$: temperature of 10% weight loss; t_{max}: temperature of maximum mass loss rate.

Table 4. TGA data of PP and PP-HNTs resins measured in air.

Sample	$w_{(HNT)}$/ ppm	$t_{0.05}$/°C	$t_{0.1}$/°C	t_{max}/°C
PP	0	230	240	277
PP-HNTs	43	234	245	304
PP-HNTs	73	257	272	378
PP-HNTs	168	246	260	370

$t_{0.05}$: temperature of 5% weight loss; $t_{0.1}$: temperature of 10% weight loss; t_{max}: temperature of maximum mass loss rate.

Table 5. Data of mechanical properties of PP-HNT resins.

Sample	$w_{(HNT)}$ (ppm)	$M_\eta \cdot 10^4$ (g·mol^{-1})	Tensile yield strength (MPa)	Young's modulus (MPa)	Elongation-at-break (%)	Flexural modulus (MPa)	Izod impact strength (kJ·m^{-2})
Control-1	0	28.8	34.7±0.6	600.7±43.6	824±68	1111±38	1.86±0.60
1	20	28.0	37.5±1.8	788.1±17.2	690±45	1191±35	1.94±0.51
3	56	31.2	40.9±1.4	807.7±45.6	754±36	1453±40	2.20±0.12
5	168	29.7	38.6±2.2	698.9±47.1	116±71	1298±44	2.15±0.45

6(c) shows the whole thermal oxidation process, and Figure 6(d) shows the partial magnification of the oxidation induction stage. It can be seen from Figure 6(c) that the oxidation rate of PP-HNTs with 73ppm and 168ppm HNTs significantly reduced. The oxidation induction time (OIT) of PP-HNTs resin shown in Figure 6(d) are almost the same with that of PP, indicating that the doping of HNTs into PP in situ do not worsen thermal oxygen aging behavior.

The mechanical property is crucial for the application of polymer, and influenced by the molecular weight and microstructure. So, the stress-strain curves and the data of mechanical properties of PP and PP-HNTs resin with same molecular weight are shown in Figure 7 and Table 5. It is found that the introduction of a small amount of HNTs (ppm level) into PP resin in situ can effectively improve the mechanical properties of the resin. In particular, compared with PP, the Young's modulus, tensile yield strength, flexural modulus and impact strength of PP-HNTs resin (Sample 3) have increased by 34%, 18%, 31% and 18%, respectively. Besides, the increase in tensile yield strength and Young's modulus approached the maximum values reported in literature [34-36]. All the improvement of mechanical properties can be related to the percolation network and the nano-enhancement effect of HNTs in PP-HNTs resin. Compared to sample 3, the slight decrease of the mechanical properties of sample 5 can be attributed to the slight decrease of the molecular weight of polymer.

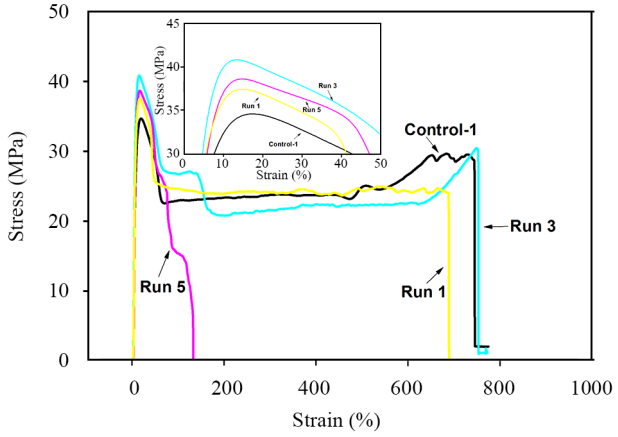

Figure 7. Stress-strain curves of PP and PP-HNTs resins.

CONCLUSION

In summary, Ziegler-Natta catalyst functionalized by doping inorganic nanoparticles was synthesized in situ. Polypropylene resins (PP-HNTs) containing ppm level halloysite nanotubes were prepared using HNTs-doped Ziegler-Natta catalyst. HNTs were dispersed in PP matrix uniformly and it was found that the PP-HNTs resins exhibited profoundly improved mechanical and thermal stability properties compared with pristine PP. The percolation network of HNTs in polymer made the mechanical enhancement more significant. The improved thermal stability of polymers is mainly due to the fact that well-dispersed HNTs exert a barrier effect for mass and heat conduction. The percolation network of HNTs also improved anti-sagging and melt processing properties of PP-HNTs resins. The preparation of PP-based nanocomposites using Ziegler-Natta catalyst doped with nanoparticles provides a facile way to relieve the contradiction between the high activity of catalyst and high content of nanoparticles, and a new idea to prepare polyolefin nanocomposites by in-situ polymerization.

CONFLICTS OF INTEREST

The authors declare that they have no known competing financial interests or personal relationship that could have appeared to influence the work reported in this paper.

ACKNOWLEDGEMENTS

This research was supported by Fundamental Research Program of Shanxi Province (Grant No. 20210302124484).

REFERENCES

1. Ning NY, Yin QJ, Luo F, Zhang Q, Du R, Fu Q (2007) Crystallization behavior and mechanical properties of polypropylene/halloysite composites. Polymer 48: 7374-7384
2. Seo MK, Lee JR, Park SJ (2005) Crystallization kinetics and interfacial behaviors of polypropylene composites reinforced with multi-walled carbon nanotubes. Mater Sci Eng A 404: 79-84
3. Lin Z, Peng M, Zheng Q (2004) Isothermal crystallization behavior of polypropylene catalloys. J Appl Polym Sci 93: 877-882
4. Taniike T, Toyonaga M, Terano M (2014) Polypropylene-grafted nanoparticles as a promising strategy for boosting physical properties of polypropylene-based nano-composites. Polymer 55: 1012-1019
5. Zhu GM, Qian DF (2001) Research progress in polymer-based nanocomposites. New Chem Mater 29: 16-21
6. Maira B, Chammingkwan P, Terano M, Taniike T (2015) New reactor granule technology for highly filled nanocomposites: effective flame retardation of polypropylene/magnesium hydroxide nanocomposites. Macromol Mater Eng 300: 679-683
7. Maira B, Chammingkwan P, Terano M, Taniike T (2017) Reactor granule technology for fabrication of functionally advantageous polypropylene nanocomposites with oxide nanoparticles. Compos Sci Tech 144: 151-159
8. Yang KF, Huang Y, Dong JY (2007) Efficient preparation of isotactic polypropylene/ montmorillonite nanocomposites by in situ polymerization technique via a combined use of functional surfactant and metallocene catalysis. Polymer 48: 6254-6261
9. Huang YJ, Qin YW, Wang N, Zhou Y, Niu H, Dong JY, Hu JP, Wang YX (2012) Reduction of graphite oxide with a grignard reagent for facile in situ preparation of electrically conductive polyolefin/graphene nanocomposites. Macromol Chem Phys 213: 720-728
10. Huang Y, Yang KF, Dong JY (2007) An in situ matrix functionalization approach to structure stability enhancement in polyethylene/ montmorillonite nanocomposites prepared by intercalative polymerization. Polymer 48: 4005-4014
11. Kaminsky W, Funck A, Wiemann K (2006) Nanocomposites by in situ polymerization of olefins with metallocene catalysts. Macromol Symp 239: 1-6
12. Wang N, Qin Y, Huang Y, Niu H, Dong JY, Wang Y (2012) Functionalized multi-walled carbon nanotubes with stereospecific Ziegler-Natta catalyst species: Towards facile in situ preparation of polypropylene nanocomposites. Appl Catal A-Gen 435-436: 107-114
13. Huang Y, Qin Y, Zhou Y, Niu H, Yu ZZ, Dong JY (2010) Polypropylene/graphene oxide nanocomposites prepared by in situ Ziegler-Natta polymerization. Chem Mater 22: 4096-4102
14. Qin Y, Wang N, Zhou Y, Huang Y, Niu H, Dong JY (2011) Fabrication of nanofillers into a granular "nanosupport" for Ziegler-Natta catalysts: towards scalable in situ preparation of polyolefin nanocomposites. Macromol Rapid Commun 32: 1052-1059
15. Du ML, Guo BC, Jia DM (2010) Newly emerging applications of halloysite nanotubes: A review. Polym Int 59: 574-582
16. Lvov Y, Abdullayev E (2013) Functional polymer-clay nanotube composites with sustained release of chemical agents. Prog Polym Sci 38: 1690-1719
17. Hendricks SB (1938) Crystal structures of the clay mineral hydrates. Nature 142: 38
18. Joussein E, Petit S, Churchman J, Theng B, Righi D, Deivaux B (2005) Halloysite clay minerals-A review. Clay Minerals 40: 383-426
19. Liu M, Jia Z, Jia D, Zhou C (2014) Recent advance in research on halloysite nanotubes-polymer nanocomposite. Prog Polym Sci 39: 1498-1525
20. Alhuthali A, Low IM (2013) Water absorption, mechanical, and thermal properties of halloysite nanotube reinforced vinyl-ester nanocomposites. J Mater Sci 48: 4260-4273
21. Handge UA, Hedicke-Höchstötter K, Altstädt V (2010) Composites of polyamide 6 and silicate nanotubes of the mineral halloysite: Influence of molecular weight on thermal, mechanical and rheological properties. Polymer 51: 2690-2699
22. Gualtieri AF (2001) Synthesis of sodium zeolites from a natural halloysite. Phys Chem Miner 28: 719-728
23. Klimkiewicz R, Drag EB (2004) Catalytic activity of carbonaceous deposits in zeolite from halloysite in alcohol conversions. J Phys Chem

Solids 65: 459-464
24. Rong TJ, Xiao JK (2002) The catalytic cracking activity of the kaolin-group minerals. Mater Lett 57: 297-301
25. Yuan P, Tan D, Annabi-Bergaya F, Yan W, Fan M, Liu D, He H (2012) Changes in structure, morphology, porosity, and surface activity of mesoporous halloysite nanotubes under heating. Clay Clay Min 60: 561-573
26. Ali M A, Betlem B, Roffel B, Weickert G (2006) Hydrogen response in liquid propylene polymerization: towards a generalized model. AIChE 52: 1866-1876
27. Abedi S, Daftari-Besheli M, Shafiei S (2005) Highly active Ziegler-Natta catalyst for propylene polymerization. J Appl Polym Sci 97: 1744-1749
28. Bangarusampath DS, Ruckdäschel H, Altstädt V, Sandler JKW, Garray D, Shaffer MSP (2009) Rheology and properties of melt-processed poly(ether ether ketone)/multi-wall carbon nanotube composites. Polymer 50: 5803-5811
29. Ma Z, Wang J, Gao X, Ding T, Qin Y (2012) Application of halloysite nanotubes. Prog Chem 24: 275-283
30. Wu D, Wu L, Zhang M, Zhao Y (2008) Viscoelasticity and thermal stability of polylactide composites with various functionalized carbon nanotubes. Polym Degrad Stabil 93: 1577-1584
31. Du ML (2007) Study on the structure and properties of polypropylene/halloysite nanotube composites. PhD Thesis, South China University of Technology
32. Kim JR, Kim YA, Yoon JH, Park DW, Woo HC (2002) Catalytic degradation of polypropylene effect of dealumination of clinoptilolite catalyst. Polym Degrad Stabil 75: 287-294
33. Park DW, Hwang EY, Kim JR, Choi JK, Kim YA, Woo HC (1999) Catalytic degradation of polyethylene over solid acid catalysts. Polym Degrad Stabil 65: 193-198
34. Garcia M, Van Vliet G, Jain SH, Schrauwen BAG, Sarkissov AU, Van Zyl WE, Boukamp BA (2004) Polypropylene/SiO_2 nanocomposites with improved mechanical properties. Rev Adv Mater Sci 6: 169-175
35. Rong MZ, Zhang MQ, Zheng YX, Zeng HM, Walter R, Friedrich K (2001) Structure–property relationships of irradiation grafted nano-inorganic particle filled polypropylene composites. Polymer 42: 167-183
36. Taniike T, Toyonaga M, Terano M (2014) Polypropylene-grafted nanoparticles as a promising strategy for boosting physical properties of polypropylene-based nanocomposites. Polymer 55: 1012-1019